Hydrol. Earth Syst. Sci. Discuss., 9, 4001–4043, 2012
www.hydrol-earth-syst-sci-discuss.net/9/4001/2012/
doi:10.5194/hessd-9-4001-2012

Hydrology and Earth System Sciences Discussions

Integrated hydrological modelling of small- and medium-sized water storages with application to the upper Fengman Reservoir Basin of China

C. Zhang[1], Y. Peng[1], J. Chu[1], and C. A. Shoemaker[2]

[1]Institute of Water Resources and Flood Control, Dalian University of Technology, Dalian 116024, China
[2]Department of Civil and Environmental Engineering, Cornell University, NY 14850, USA

Received: 31 January 2012 – Accepted: 24 February 2012 – Published: 28 March 2012

Correspondence to: Y. Peng (pyongcuidi@163.com)

Published by Copernicus Publications on behalf of the European Geosciences Union.

Abstract

Hydrological simulation in regions with a large number of water storages is difficult due to the inaccurate water storage data, including both topologic parameters and operational rules. To address this issue, this paper presents an improved version of SWAT2005 (Soil and Water Assessment Tool, version 2005) using the satellite-based dataset Landsat, an empirical storage classification method, and some empirical relationships to estimate water storage and release from the various levels of flow regulation facilities. The improved SWAT2005 is characterised by three features: (1) a realistic representation of the relationships between the water surface area and volume of each type of water storage, ranging from small-sized ponds for water flow regulation to large-sized and medium-sized reservoirs for water supply and hydropower generation; (2) water balance and transport through a network combining both sequential and parallel streams and storage links; and (3) calibrations for the physical parameters and the human interference parameters. Both the original and improved SWAT2005 are applied to the upper Fengman Reservoir Basin, and the results of these applications are compared. The improved SWAT2005 accurately models small- and medium-sized storages, indicating a significantly improved performance from that of the original model in reproducing streamflows.

1 Introduction

Water storages, including reservoirs and ponds, are important management tools in the exploitation and utilisation of water resources (Gross and Moglen, 2007; Lopez-Moreno et al., 2009). The small- and medium-sized water storages mentioned in this study refer to small- and medium-sized reservoirs and ponds.

Different approaches have been developed to account for the impacts of water storages on runoff in hydrological simulations. Individual water storage simulation models (e.g. Jayatilaka et al., 2003; Saxton and Willey, 2004) have been developed for

HESSD
9, 4001–4043, 2012

small-sized river catchments. The results of previous studies suggest that these models could be used to develop a useful tool for optimising the usage of limited water resources in similar regions with a small amounts of water storages, i.e. less than ten interconnected water storages.

Distributed, physically based models such as SWAT2005 (Neitsch et al., 2002a, c) are typically used for the hydrological simulation of large-sized river catchments. SWAT2005 uses hydrological responding units (hrus) as the basic modelling units to explicitly consider the water storages by appropriately parameterising their corresponding hrus (Payan et al., 2008). For example, to assess the impacts of water storages on streamflow in the Huai River Basin of China, Wang and Xia (2010) spatially represented 61 water storages in SWAT2000 by modifying the outflow calculation method for water storages. However, distributed, physically based models often require a great amount of input data and intensive computation due to the small scales of measurements, such as hrus for SWAT2005 (Sophocleous and Perkins, 2000).

To reduce the computational requirement, Payan (2008) proposed a way to account for man-made reservoirs in a lumped hydrological model. This model could not explicitly simulate the key processes in reservoirs (infiltration, evaporation, operation, and so on); instead, it used the observed volume variations to represent these processes. Obviously, the model simplifications may not reasonably reflect various reservoir processes, particularly those in a large-scale, complex river catchment.

To represent several thousands of reservoirs located in the State of Ceará in semi-arid Northeast Brazil, Güntner et al. (2004) presented a simple deterministic water balance modelling scheme within a distributed model. The key component of the scheme was a cascade-type approach, within which the reservoirs were grouped into six classes according to storage capacity, each with different rules for flow routing. Water uses were considered for irrigation and livestock, as well as domestic, industrial and tourist uses. The scheme assumed that the smaller-sized reservoirs were located upstream of larger-sized reservoirs and that the outflows from smaller-sized reservoirs were equally discharged into all of the larger-sized reservoir classes located

HESSD
9, 4001–4043, 2012

downstream. To cope with data scarcity, particularly regarding water use and water surface area, the scheme used empirical data of water use and an empirical formula to calculate water surface area. Additionally, reservoir operation rules were not considered in the scheme. Refinements of the model should primarily focus on an improved definition of the basin area fractions contributing to individual reservoir classes by using more detailed data on topography and reservoir locations from remote sensing studies. Furthermore, a better knowledge of reservoir operation rules promises to significantly improve the model's performance.

Therefore, the basin hydrologic cycle must be simulated accurately with all of the available information and reasonable modelling simplifications of the numerous water storages in catchments with a large number of water storages. Given the limitations of SWAT2005, the aim of this paper is to present an improved version of SWAT2005 to allow water storages in a large-scale river catchment to be simulated more accurately. There have been several studies on obtaining the surface areas of small-sized reservoirs with satellite images (White, 1978; McFeeters, 1996; Frazier and Page, 2000). Optical (i.e. Landsat, Spot, Aster and ISS) or radar satellite systems (i.e. Envisat, ERS, and Radarsat) could be used to obtain the surface areas of small-sized reservoirs. Envisat ASAR (C-band radar) and Landsat TM/ETM+ data (multispectral imagery) now provide images at spatial resolutions of 30 and 15 m, respectively (Gardini et al., 1995). In India, the storage volumes of small-sized reservoirs were estimated with Landsat images (Mialhe et al., 2008). Envisat advanced synthetic aperture radar (ASAR) was used to obtain the surface areas of reservoirs (Liebe et al., 2009). The main characteristics of the improved SWAT2005 are summarised as follows: (1) a realistic representation of the relationships between the water surface area and volume of each type of water storages, ranging from ponds for water regulation to large- and medium-sized reservoirs for water supply and hydropower generation with the satellite-based dataset Landsat; (2) water balance and transport through a network combining both sequential and parallel streams and storage links to more accurately define the basin area fractions contributing to individual water storage classes; and (3) calibrations for the

HESSD
9, 4001–4043, 2012

physical parameters and the human interference parameters to gain a better understanding of reservoir operation rules.

The improved SWAT2005 is applied to the upper Fengman Reservoir Basin, which has many small- and medium-sized water storages for irrigation, industrial, and domestic uses. The impoundment and release of these storages have a significant influence on the inflows to the Fengman Reservoir, thus making the Fengman Reservoir increasingly difficult to operate, particularly during flood seasons. During non-flood seasons and the preliminary stage of a flood season, inflows to the Fengman Reservoir are reduced due to the impoundment of water storages, and power generation is affected. In the middle of flood seasons, inflows to the Fengman Reservoir increase due to the release of water storages, and flood control is affected. There are so many small- and medium-sized water storages in the upper Fengman Reservoir Basin that it is difficult to obtain their detailed design and running information. Furthermore, computing time increases substantially when all of the water storages in the upper Fengman Reservoir Basin are added to the models. The simulation results from the improved SWAT2005 model small- and medium-sized water storages more accurately than the original SWAT2005.

2 Methodologies

The framework for the improved SWAT2005 is shown in Fig. 1, and the grey area is the location of the improvements.

In view of the hundreds or thousands of water storages that may be located in a large-scale river catchment, it is not feasible to describe each water storage individually in a large-scale model. Thus, the focus of this paper is not to exactly represent the behavior of each water storage, but rather to accurately model the water storage system on an aggregated level to allow water storages in a large-scale river catchment to be more accurately simulated. Detailed design and running information are known for all large- and medium-sized reservoirs. For small-sized reservoirs, only their geographic

HESSD
9, 4001–4043, 2012

positions, drainage areas, emergency storage volumes, and principal storage volumes are known at the level of administrative units (municipalities). For ponds, only their total drainage areas and storage volumes are known at the basin level. Therefore, water storages are grouped into $r_{max} = 5$ classes depending on their storage capacities V_{max} (Table 1). Large-sized reservoirs are the water storages of class 5, medium-sized reservoirs are the water storages of class 4, small-sized reservoirs are the water storages of classes 2 and 3 based on their storage capacities, and ponds are the water storages of class 1.

SWAT is a nearly ideal model for basin-scale water resources applications due to its reservoir and pond modules. SWAT has been widely used in a variety of investigations, such as hydrological simulation and assessment, non-point pollution, climate change impact, parameter sensitivity, and model calibration and uncertainty analysis (Borah and Bera, 2004; Arnold and Fohrer, 2005; Gassman et al., 2007).

The water balance used in the reservoir and pond modules to simulate water storages is

$$V = V_{store} + V_{flowin} - V_{flowout} + V_{pcp} - V_{evap} - V_{seep} \quad (1)$$

where V is the volume of water in reservoirs and ponds at the end of the day (m^3); V_{stored} is the volume of water stored in reservoirs and ponds at the beginning of the day (m^3); V_{flowin} is the volume of water entering reservoirs and ponds during the day (m^3); V_{pcp} is the volume of precipitation falling on reservoirs and ponds during the day (m^3); V_{evap} is the volume of water removed from reservoirs and ponds by evaporation during the day (m^3); and V_{seep} is the volume of water lost from reservoirs and ponds by seepage during the day (m^3).

The surface areas of water storages are needed to calculate the amount of precipitation falling on water storages and the amount of evaporation and seepage removed from water storages in SWAT. Surface area varies with the water volume of the water storages.

HESSD
9, 4001–4043, 2012

In SWAT2005, surface area is updated daily using the following equations

$$SA = \beta_{sa} \cdot V^{exsa} \tag{2}$$

$$exsa = \frac{\log_{10}(SA_{em}) - \log_{10}(SA_{pr})}{\log_{10}(V_{em}) - \log_{10}(V_{pr})} \tag{3}$$

$$\beta_{sa} = \left(\frac{SA_{em}}{V_{em}}\right)^{exsa} \tag{4}$$

where SA is the surface area of the water storage (ha); V is the volume of water in the water storage (m^3); SA_{em} is the surface area of the water storage when filled to the emergency spillway (ha); SA_{pr} is the surface area of the water storage when filled to the principal spillway (ha); V_{em} is the volume of water held in the water storage when filled to the emergency spillway (m^3); and V_{pr} is the volume of water held in the water storage when filled to the principal spillway (m^3).

Güntner et al. (2004) calculated water surface area as a function of the actual storage volume with

$$A_{RL} = c_{RL} \cdot (V_t)^{d_{RL}} \tag{5}$$

where c_{RL} and d_{RL} are reservoir-specific constants depending on its geometry.

Liebe et al. (2005) estimated storage volume as a function of surface area with

$$V = 0.00857 \cdot A_{Res}^{1.4367} \tag{6}$$

where V is the volume of the water storage (m^3), and A_{Res} is its area (m^2).

Because the surface area of a water storage is related to its scope, storage and drainage area, the relationship between surface area and storage volume varies for the different water storage classes. It is not reasonable to use a definite relationship between surface area and storage volume to calculate the surface areas of different water storage classes, as done previously by Güntner et al. (2004), Liebe et al. (2005) and SWAT2005. In this paper, an approach for obtaining more precise relationships

HESSD
9, 4001–4043, 2012

between the surface area and storage volume of different water storage classes is proposed.

Water balance and transport through a network combining both sequential and parallel streams and storage links is proposed, incorporating surface runoff and routing mechanisms based on the spatial topological relationships among water storages, water impoundment and the release regulations of water storages with water uses.

The reservoir module in SWAT can simulate water storages with detailed design and running information. The pond module in SWAT is an aggregate model of water bodies within any sub-basin. Therefore, in this paper, minor large- and medium-sized reservoirs (classes 4 and 5) are added to SWAT2005 and simulated by the reservoir module of SWAT2005. Small-sized reservoirs and ponds (classes 1–3) are not added to SWAT2005; instead, they are simulated by the pond module of SWAT2005. The pond module of SWAT2005 treats all small-sized reservoirs and ponds within a sub-basin as one water storage, and surface runoff and routing processes among the storages are not considered. Obviously, the pond module of SWAT2005 is a reasonable simplification but must be improved to more accurately simulate large catchments.

Water consumption is considered to be lost from the system. SWAT allows water to be removed from the shallow aquifer, the deep aquifer, the reach, or the water storage within any sub-basin. Water consumption is allowed to vary from month to month. The average daily volume of water removed from the source needs to be specified for each month. Because the related water-use data, such as source location, are difficult to collect and variable for water uses in different places and during different years, the water-use distribution approach is proposed in this paper.

Because numerous water storages within the basin significantly influence the basin's hydrologic cycle, the impacts of water storages must be included in the parameters and calibrated in the hydrological simulation process with hydrological models. Therefore, calibration of the physical parameters and then the human interference parameters is proposed in the parameter calibration process to allow the water storages in a large-scale river catchment to be more accurately simulated.

HESSD
9, 4001–4043, 2012

2.1 Relationships between water surface area and storage volume for water storages

2.1.1 Surface area

The principal storage volumes and emergency storage volumes of water storages were collected from the Hydrological Administration of Jilin Province in China. In this paper, the reservoir surface areas are extracted from Landsat TM/ETM+ data from 1986 to 2006 with the bands relationship. The Landsat TM/ETM+ data are collected from the International Science Data Service Platform (http://datamirror.csdb.cn). Because Landsat TM/ETM+ provides high-resolution spatial data for every 16 days, the Landsat TM/ETM+ data for flood seasons in wet years are used to extract the surface areas of water storages within the basin. The extracted surface areas of flood seasons in wet years are assumed to correspond with the water storages' principal storage volumes. Because 2005 is a wet year and the flood season is from June to August, Landsat TM/ETM+ data from 9 September 2005, are used to extract the surface areas of the water storages within the basin.

2.1.2 Classifications of water storages and relationship between water surface area and principal storage volume for each water storage class

Water storages with different slopes, storages, and drainage areas have different relationships between their surface area and storage volume. Therefore, the three elements (slope, storage, and drainage area) should be considered when developing the relationships between water surface area and principal storage volume for each water storage class. The ratio of drainage area to storage volume (drainage area/storage volume) is set as an index to classify water storages. For larger ratios, the storage volume increases more rapidly and there is a higher probability of reaching the principal storage volume during wet periods. The approach to classifying water storages and acquiring the relationships between water surface area and principal storage volume for each water storage class is described below.

HESSD
9, 4001–4043, 2012

Step 1 Set the water storages' initial classifications according to the value distributions of their classification indexes (slope, drainage area/storage volume, and principle storages).

Step 2 Calculate each water storage class' mean characteristics, such as the mean storage volume, mean drainage area, and mean slope, and find the medium-sized reservoir in the basin with similar mean characteristics. Because detailed design and running information are known for the medium-sized reservoirs, use the ratio of the storage volume of the medium-sized reservoir from 9 September 2005, to its principle storage volume to adjust the principle storage volume of the water storages in the water storage class.

Step 3 Calculate the correlation coefficients between the water surface area and principal storage volume of the water storages for each water storage class.

Step 4 Adjust the classification indexes and repeat step 2 until the correlation coefficients no longer improve.

2.2 Water balance and transport through a network combining both sequential and parallel streams and storage links

In this paper, a sequential and parallel routing scheme is developed to approximately describe the upstream-downstream positions of different water storage classes within the sub-basin and the redistribution of runoff among them. The major difference between the cascade scheme and the sequential and parallel routing scheme is the way in which the inflow and outflow of water storages are calculated. More specifically, the latter divides the water storages into two simulation classes: classes 4–5 (large- and medium-sized reservoirs) and classes 1–3 (small-sized reservoirs and ponds). Additionally, to show the variabilities of water uses in different places and during different years, the water-use distribution approach based on parameter calibration is proposed and presented below.

HESSD
9, 4001–4043, 2012

2.2.1 Large- and medium-sized reservoirs

The water balance for large- and medium-sized reservoirs is represented explicitly by the reservoir module of SWAT2005 because (1) they are of great importance to water supplies and (2) they are the only reservoirs with detailed reservoir characteristics. The location of their dams is the criterion by which the entire basin is subdivided into sub-basins that are linked via the river network.

2.2.2 Small-sized reservoirs and ponds

The pond module of SWAT2005 is improved in this paper. The large number of small-sized reservoirs and countless ponds (classes 1–3) are represented in the improved SWAT2005 in an aggregated manner (Fig. 2).

– Simplification and spatial distribution

  Because the geographic position of each small-sized reservoir is known, the spatial topology of small-sized reservoirs within an individual sub-basin is determined. From a detailed survey of the spatial topology of small-sized reservoirs in an individual sub-basin, it is reasonable to assume that small-sized reservoirs of the same class are interconnected in a parallel scheme, and small-sized reservoirs of different classes are interconnected in a sequential scheme (Fig. 2).

  Given that the number, n_r, of water storages in each class, r, is known for each sub-basin, the water balance of each water storage class, r, within each sub-basin is calculated for one hypothetical representative reservoir, RM, with the mean characteristics for that water storage class within the corresponding sub-basin, i.e. with its storage capacity being equal to the mean value of the water storages belonging to that class in the corresponding sub-basin. The water balance of RM within each sub-basin was calculated with a daily time step according to

$$V_{\mathrm{RM}r,t} = V_{\mathrm{RM}r,t-1} + \frac{Q_{\mathrm{in},r}}{n_r} - Q_{\mathrm{out,RM}r} + V_{\mathrm{pcp,RM}r} - V_{\mathrm{evap,RM}r} - V_{\mathrm{seep,RM}r} \quad (7)$$

HESSD
9, 4001–4043, 2012

where $V_{RMr,t}$ is the storage volume of the hypothetical mean reservoir RM in water storage class r at day t; $Q_{in,r}$ is the daily inflow to water storage class r; n_r is the number of water storages in class r; $Q_{out,RMr}$ is the daily outflow from reservoir RM; $V_{pcp,RMr}$ is the daily precipitation to reservoir RM's water surface; and $V_{evap,RMr}$ and $V_{seep,RMr}$ are the daily evaporation and seepage from reservoir RM, respectively (all in m^3). The values of $V_{pcp,RMr}$, $V_{evap,RMr}$, and $V_{seep,RMr}$ are calculated with SWAT2005, and the total actual storage volume $V_{r,t}$ of water storage class r within each sub-basin is obtained by

$$V_{r,t} = V_{RMr,t} \cdot n_r \quad (8)$$

– Inflow

The total sub-basin area is distributed as runoff contributing areas among the different water storage classes according to their drainage areas. The inflow $Q_{in,r}$ of water storage class r comprises direct inflow and additional inflow. The direct inflow to water storage class r is the fraction fr_r of the total sub-basin runoff Q_{gen} and is generated in a time step as the difference between the fraction fr_r of the sub-basin area that drains into water storage class r and the fraction fr_x of the sub-basin area that drains into water storage class $x < r$ within the drainage of water storage class r. Additional inflow to a water storage class r is provided by the fraction fr_r of outflow $Q_{out,x}$ of all water storage classes $x < r$ within the drainage of water storage class r. This approach accounts for the fact that a water storage could be upstream of any larger water storage (not necessarily a water storage of the next larger class) and have no other smaller water storage in the downstream direction. Additionally, outflow from one water storage class is attributed to any larger water storage class within the sub-basin in the same time step.

– Inflow of class 1

The pond category (class 1) is located on the top of the sequential and parallel routing scheme for water storages. The inflow of class 1 is the runoff

HESSD
9, 4001–4043, 2012

generated in its drainage.

$$Q_{\text{in},1} = \text{fr}_1 \cdot Q_{\text{gen}} \quad (9)$$

– Inflow of class 2

The inflow of class 2 is the sum of its direct inflow and additional inflow. Its direct inflow is the difference between the runoff generated in the drainage of class 2 and that generated in the drainage of class 1 within the drainage of class 2. Its additional inflow is the outflow of class 1 within the drainage of class 2.

$$Q_{\text{in},2} = (1 - \text{fr}_1) \cdot \text{fr}_2 \cdot Q_{\text{gen}} + \text{fr}_2 \cdot Q_{\text{out},1} \quad (10)$$

– Inflow of class 3

The inflow of class 3 is the sum of its direct inflow and additional inflow. Its direct inflow is the difference between the runoff generated in the drainage of class 3 and that generated in the drainage of classes 1 and 2 within the drainage of class 3. Its additional inflow is the outflow of classes 1 and 2 within the drainage of class 3. However, the runoffs generated in the drainage of class 1 within the drainage of class 2 and the outflows of class 1 within the drainage of class 2 are not considered.

$$Q_{\text{in},3} = (1 - \text{fr}_1 - \text{fr}_2 + \text{fr}_1 \cdot \text{fr}_2) \cdot \text{fr}_3 \cdot Q_{\text{gen}} + \text{fr}_3 \cdot (Q_{\text{out},1} + Q_{\text{out},2} - \text{fr}_2 \cdot Q_{\text{out},1}) \quad (11)$$

– Outflow

Because classes 1–3 (small-sized reservoirs and ponds) are simulated with the pond module of SWAT2005, they are referred to below as ponds. In the pond module of SWAT2005, the volume of pond outflow may be calculated with the target storage approach. The target storage varies with flood season and soil water content. The target volume is calculated as

$$V_{\text{tar}} = V_{\text{em}} \quad \text{If} \quad \text{mon}_{\text{fld,beg}} < \text{mon} < \text{mon}_{\text{fld,end}} \quad (12)$$

HESSD
9, 4001–4043, 2012

$$V_{tar} = V_{pr} + \frac{\left(1 - \min\left[\frac{SW}{FC}, 1\right]\right)}{2} \cdot (V_{em} - V_{pr}) \quad (13)$$

If $mon \le mon_{fld,beg}$ or $mon \ge mon_{fld,end}$

where V_{tar} is the target pond volume for a given day (m^3); V_{em} is the volume of water held in the pond when filled to the emergency spillway (m^3); V_{pr} is the volume of water held in the pond when filled to the principal spillway (m^3); SW is the average soil water content in the sub-basin (mm); FC is the water content of the sub-basin soil at field capacity (mm); mon is the month of the year; $mon_{fld,beg}$ is the beginning month of the flood season; and $mon_{fld,end}$ is the ending month of the flood season.

Once the target storage is defined, the pond outflow is calculated as

$$V_{flowout} = \frac{V - V_{tar}}{ND_{tar}} \quad (14)$$

where $V_{flowout}$ is the volume of water flowing out of the pond during the day (m^3); V is the volume of water stored in the pond (m^3); V_{tar} is the target pond volume for a given day (m^3); and ND_{tar} is the number of days required for the pond to reach its target storage.

The outflow regulations of ponds are not considered in the target storage calculation. Güntner et al. (2004) assumed that outflows from the small- and medium-sized reservoirs only occur if the storage capacities are exceeded. Because the small-sized reservoirs within the study area presented in Güntner et al. (2004) were mainly simple earth dams without any outflow regulation devices, the outflow calculations proposed by Güntner et al. (2004) were valid. However, in China, different outflow regulations are used in the different pond classes (classes 1–3) and during the different periods, including the non-flood season, the beginning

HESSD
9, 4001–4043, 2012

of the flood season, the middle of the flood season, and the end of the flood season. Due to the lack of information on outflow regulations, in the target storage calculation, four principal storage volume adjustment parameters are set for the non-flood season, the beginning of the flood season, the middle of the flood season, and the end of the flood season.

– Target storage for class 1

$$V_{tar} = V_{em} \tag{15}$$

– Target storage for classes 2 and 3

$$V_{tar} = \beta_{fld,beg} \cdot V_{pr} \tag{16}$$

If May < mon < Jun (the beginning of the flood season)

$$V_{tar} = \beta_{fld,mid} \cdot V_{pr} \quad \text{If} \quad \text{Jul} < \text{mon} < \text{Aug} \quad \text{(the middle of the floodseason)} \tag{17}$$

$$V_{tar} = \beta_{fld,end} \cdot V_{pr} \quad \text{If} \quad \text{Sept} < \text{mon} < \text{Oct} \quad \text{(the end of the flood season)} \tag{18}$$

$$V_{tar} = \beta_{nonflod} \cdot V_{pr} + \frac{\left(1 - \min\left[\frac{SW}{FC}, 1\right]\right)}{2} \cdot (V_{em} - V_{pr}) \tag{19}$$

If $\text{mon} \le \text{mon}_{fld,beg}$ or $\text{mon} \ge \text{mon}_{fld,end}$

where V_{tar}, V_{em}, V_{pr}, SW, FC, mon, $\text{mon}_{fld,beg}$, and $\text{mon}_{fld,end}$ have been described above and $\beta_{fld,beg}$, $\beta_{fld,mid}$, $\beta_{fld,end}$, and $\beta_{nonflod}$ are the four principal storage volume adjustment parameters set for the beginning of the flood season, the middle of the flood season, the end of the flood season, and the non-flood season, respectively.

2.2.3 Water-use distribution based on the parameter calibration

If the detailed water-use data of a given year are treated as the baseline, the water-use data of each sector (irrigation, livestock, domestic, industrial, and tourist water

HESSD
9, 4001–4043, 2012

use) are distributed spatially and temporally with land use and annual precipitation, respectively. Referred to the sources of water uses, six fraction parameters are set for the three sources (water storages, reaches, and shallow aquifers) during two separate time periods (October to April and May to September), i.e. $\alpha_{pnd,octapr}$ and $\alpha_{pnd,maysep}$ are set for the water storages in October to April and May to September, respectively, $\alpha_{rch,octapr}$ and $\alpha_{rch,maysep}$ are set for the reaches in October to April and May to September, respectively, and $\alpha_{gw,octapr}$ and $\alpha_{gw,maysep}$ are set for the shallow aquifers in October to April and May to September, respectively.

2.3 Physical parameter and human interference parameter calibrations

2.3.1 Calibration approach

The physical parameter calibration is first processed with minimal human activities. The human activity parameter calibration is then processed with stable human activities. Distinguish the natural and stable periods, apply the parameters calibrated during the natural period to the hydrological simulation during the stable period, and avoid the phenomenon of "the same effect of different parameters". In this paper, the sensitivity analysis and calibration helper module of SWAT2005 are used to calibrate the parameters during the two periods.

2.3.2 Evaluation criterion

The mean relative error (MRE), the coefficient of determination (R^2), and the Nash-Sutcliffe efficiency (NSE) are used to evaluate the simulated streamflows with the observed streamflows.

The MRE is computed according to Eq. (20).

$$\mathrm{MRE} = \frac{P^{\mathrm{mean}} - Q^{\mathrm{mean}}}{Q^{\mathrm{mean}}} \times 100\% \quad (20)$$

HESSD
9, 4001–4043, 2012

where P^{mean} and Q^{mean} are the means of the simulated streamflows and the observed streamflows, respectively. "MRE values of 0 indicate a perfect fit. Positive values indicate model overestimation bias, and negative values indicate model underestimation bias (Hao et al., 2006)."

R^2 is computed according to Eq. (21).

$$R^2 = \frac{\sum_{i=1}^{n}\left(P_t - P^{\text{mean}}\right)\left(Q_t - Q^{\text{mean}}\right)}{\sqrt{\sum_{i=1}^{n}\left(P_t - P^{\text{mean}}\right)^2 \sum_{i=1}^{n}\left(Q_t - Q^{\text{mean}}\right)^2}} \tag{21}$$

where P_t is the ith simulated value for the streamflows; Q_t is the ith observation for the streamflows; P^{mean} is the mean of the simulated streamflows; Q^{mean} is the mean of the observed streamflows; and n is the total number of observations. "R^2 describes the portion of the variance in measured data explained by the model. R^2 ranges from 0 to 1, with lower values indicating more error variance, and typically $R^2 = 1$ is considered the optimal value (Moriasi et al., 2007)."

NSE is computed according to Eq. (22).

$$\text{NSE} = 1 - \frac{\sum_{i=1}^{n}\left(Q_t - P_t\right)^2}{\sum_{i=1}^{n}\left(Q_t - Q^{\text{mean}}\right)^2} \tag{22}$$

where Q_t is the ith observation for the streamflows; P_t is the ith simulated value for the streamflows; Q^{mean} is the mean of the observed streamflows; and n is the total number of observations. The NSE ranges between $-\infty$ and 1.0, with NSE = 1.0 as the optimal value. "*Values between 0.0 and 1.0 are generally viewed as acceptable levels of performance, whereas a value less than 0.0 shows that the mean observed value is a better predictor than the simulated value, which indicates unacceptable performance*" (Luo et al., 2008).

HESSD
9, 4001–4043, 2012

3 Datasets

3.1 Study site

The Fengman Reservoir, which has a storage volume of more than 112×10^8 m^3, is located in the Second Songhua River, situated in the southeast of Jilin province in China. Its basin drains an area of 42 500 km^2, occupying 55 % of the total drainage area of the Second Songhua River and consisting of approximately 2000 reservoirs and countless ponds. Approximate 9335 water storages, each with a water area of more than 4000 m^2, could be identified in the basin with the 2002 satellite remote sensing images. In 1995, due to impoundment and the release of water storages, the unpredictable inflows to the Fengman Reservoir were approximate 4×10^8 m^3 during the flood season. Therefore, the basin hydrologic water cycle simulation is becoming increasingly difficult, and the impact rules of impoundment and the release of water storages on runoff are difficult to obtain. Given that the Fengman Reservoir is a multipurpose reservoir serving flood control, power generation, and water supply, the Fengman Reservoir operation has become increasingly difficult recently, particularly during the flood season.

The study area is limited to the upper-middle stream region of the Fengman Reservoir above the Wudaogou hydrologic station, referred to as the Fengman Reservoir Basin in this study. The basin drains an area of 12 411 km^2. Its mean annual precipitation is 720 mm, and its mean annual precipitation during the flood season is 510 mm, accounting for more than 70 % of its mean annual precipitation. The water storages within the basin drain an area of 7421.27 km^2, accounting for 63.98 % of the basin drainage area.

Ten rain gauges (Liuhe, Huifacheng, Fumin, Hailong, Sanyuanpu, Xiangyang, Meihekou, Gushanzi, Jiangjiajie, and Yangmulin) and four hydrologic stations (Panshi, Dongfeng, Yangzishao, and Wudaogou) are within the basin (Fig. 3). The ten rain gauges provide daily precipitation data, whereas the four hydrologic stations provide daily precipitation and streamflow data. The spatial topology of water storages in the individual sub-basin above the Panshi hydrologic station (Fig. 4) justifies the assumptions

HESSD
9, 4001–4043, 2012

that small-sized reservoirs of the same class are interconnected in a parallel scheme and that small-sized reservoirs of different classes are interconnected in a sequential scheme.

Based on the survey, one large-sized reservoir (class 5), i.e. the Hailong reservoir, twelve middle-sized reservoirs (class 4), approximately 500 small-sized reservoirs (classes 2 and 3), and countless ponds (class 1) were built from the 1950s to the 1980s in the Fengman Reservoir Basin. The total storage volume of classes 2–5 is approximately 9.58×10^8 m^3. The storage volume of the Hailong Reservoir is approximately 3.70×10^8 m^3. The total storage volume of classes 2–4 is approximately 5.88×10^8 m^3. Therefore, the numerous water storages significantly influence the runoff within the basin. The drainage area and storage volume of each water storage class within the basin are shown in Table 1. The small-sized reservoirs (classes 2 and 3) have the largest drainage area and storage volume, while the numerous ponds (class 1) have the smallest storage volume. Numerous water storages were built from the 1960s to the 1990s, and a few water storages were built before 1956 or after 1990. Therefore, the pre-1956 and post-1990 periods are treated as natural and stable periods, respectively.

3.2 Data collection

Next, a short description of the data gathered for the Fengman Reservoir Basin is provided, and the way in which the data were processed for the application of the improved SWAT2005 is described.

1. DEM data (raster resolution: 90 m × 90 m) were obtained from http://srtm.csi.cgiar.org.

2. Soil data (scale = 1 : 10^6) were collected from the Data Center for Resources and Environmental Sciences Chinese Academy of Sciences (RESDC).

3. Land use data for the 1980s and 2000s (scale = 1 : 10^5) were collected from the

HESSD
9, 4001–4043, 2012

Data Center for Resources and Environmental Sciences Chinese Academy of Sciences (RESDC). Because several water storages were built before 1956 or after 1990 in the Fengman Reservoir Basin, basin land use data for the years before 1956 and after 1990 are also needed. Previous studies show that from 1954 to 1976, the main land use change was the decrease in the area of upstream mountains, and the decreased forest area was mainly used for crops and grasses (Zhang et al., 2006; Kuang et al., 2006). The population of the eastern mountain area of Jilin Province increased from 1950 to 2000. The population was 219 600 in 1954 and 2.12 times that in 1976. The population in 2000 was 2.62 times the population in 1956. Therefore, to obtain basin land use data for the years before 1956, the basin land use data for the 1980s are modified as follows: (1) the basin water storage land use is modified to forest, and (2) according to the basin population distribution, the basin grass and crop land uses in the locations, where the population in 1980 is dense and the population in 1956 is sparse are modified to forest.

4. Digital river network data (scale = $1:2.5\times10^5$) were obtained from the 1 : 4 M-scale Topographic Database of the National Fundamental Geographic Information System of China.

5. Daily precipitation data for 14 stations over a 54 yr period (1953–2006) and daily streamflow data for 4 stations over a 53 yr period (1954–2006) were obtained from the Hydrological Administration of Jilin Province, China. Daily meteorological data (temperature, solar radiation, weed speed, and relative humidity) for 4 stations over a 54 yr period (1953–2006) were obtained from the China Meteorological Data Sharing Service System.

6. All of the individual water storage characteristics were obtained from the Hydrological Administration of Jilin Province, China. Detailed design and running information are known for the large- and medium-sized reservoirs (classes 4 and 5). For small-sized reservoirs (classes 2 and 3), only their geographic positions,

HESSD
9, 4001–4043, 2012

drainage areas, emergency storage volumes, and principal storage volumes are known at the level of administrative units (municipalities). For ponds (class 1), only the total drainage area and storage volume are known at the basin level.

7. Water-use data for the 2000s were obtained from the Hydrological Administration of Jilin Province, China, and were used as a baseline.

4 Results and discussions

4.1 Results of the water storage classification and the relationship between water surface area and principal storage volume for each water storage class

The classifications and relationships between the water surface area and principal storage volume for each water storage class within the basin, obtained with the aforementioned method, are given in Table 2.

4.2 Calibration and validation results

The improved SWAT2005 is used to simulate streamflow in the Fengman Reservoir Basin. Because hydrologic stations within the basin are scarce in the streamflow data for the 1950s, the Yangzishao and Wudaogou hydrologic stations were chosen as calibration stations during the natural periods, and the streamflow data from the pre-1960 period were used to calibrate the physical parameters. Because the main human activities, taking place in the upper part of the Panshi and Dongfeng hydrologic stations were water storages, the Panshi and Dongfeng hydrologic stations were chosen as calibration stations during the stable period, and the streamflow data from the 1990–1995 period were used to calibrate the human activity parameters, and the streamflow data from the post-1996 period were used to validate the human activity parameters. The Yangzishao and Wudaogou hydrologic stations were chosen as the

HESSD
9, 4001–4043, 2012

improved SWAT2005 validation stations during the stable period, and the streamflow data from the post-1990 period were used to validate the improved SWAT2005.

To compare the performance between the original and improved SWAT2005, three scenarios are designed: S0 (considering human activities according to the original SWAT2005 with the calibrated physical parameters), S1 (considering human activities according to the improved SWAT2005 with the calibrated physical and human activity parameters described aforementioned), and S2 (considering water balance and transport through a network combining both sequential and parallel streams and storage links and ignoring the human activity parameters).

4.2.1 First-stage calibration results

Figure 5 shows the observed and simulated monthly streamflows during the physical parameter calibration period (before 1960) at the Yangzishao and Wudaogou hydrologic stations, and the calibrated physical parameters are shown in Table 3.

4.2.2 Second-stage calibration results

Figure 6 shows the observed and simulated monthly streamflows by S0 and S1 during the human activity parameter calibration period (1990–1995) at the Panshi and Dongfeng hydrologic stations, and the calibrated human activity parameters are shown in Table 4.

4.2.3 Validation results

Figure 7 shows the observed and simulated monthly streamflows by S0 and S1 over the validation periods at the Panshi, Dongfeng, Yangzishao and Wudaogou hydrologic stations. There is a clear improvement in the simulation at the Panshi and Dongfeng hydrologic stations, while the simulation at the Yangzishao and Wudaogou hydrologic stations improved less significantly. Over the validation periods, the mean model performance rises from 0.855 (R^2) and 0.665 (NSE) to 0.914 and 0.816 at the Panshi and

HESSD
9, 4001–4043, 2012

Dongfeng hydrologic stations, respectively, while the mean model performance rises from 0.922 (R^2) and 0.829 (NSE) to 0.953 and 0.903 at the Yangzishao and Wudaogou hydrologic stations, respectively.

From Fig. 7, there are six larger flood processes in the validation periods, which are in 1996, 1998, 2003, 2004, 2005, and 2006, and the years before 1998 and 2004 are drier and wetter, respectively, than average. Therefore, Fig. 8 shows the evaluation criterion for the flood seasons over the validation periods as well as the observed and simulated monthly streamflows by S0 and S1 for the 1998 and 2004 flood seasons at the Panshi, Dongfeng, Yangzishao and Wudaogou hydrologic stations. Figure 8 also shows that there is a clear improvement in the simulation at the Panshi and Dongfeng hydrologic stations, while the simulation at the Yangzishao and Wudaogou hydrologic stations improved less significantly for the flood seasons over the validation periods. For the flood seasons over the validation periods, the mean model performance rises from 0.842 (R^2) and 0.638 (NSE) to 0.916 and 0.826 at the Panshi and Dongfeng hydrologic stations, respectively, while the mean model performance rises from 0.921 (R^2) and 0.812 (NSE) to 0.956 and 0.909 at the Yangzishao and Wudaogou hydrologic stations, respectively.

Figure 9 compares the evaluation criterions of S0, S1, and S2 for the flood seasons over the validation periods at the Panshi and Dongfeng hydrologic stations. For the flood seasons over the validation periods, the mean model performance rises from 0.842 (R^2) and 0.638 (NSE) by S0 to 0.885 and 0.774 by S2 at the Panshi and Dongfeng hydrologic stations, respectively, and the R^2 and NSE in S2 are improved by 58.122 % and 72.208 %, respectively, compared to those in S1.

Figure 10 shows the water balance and transport through a network combining both sequential and parallel streams and storage links above the Panshi hydrologic station over the validation periods. The results indicated that approximately 9.0 % of the annual total inflows to small-sized reservoirs (class 2) were derived from ponds (class 1), and approximately 9.2 % and 7.7 % of the annual total inflows to small-sized reservoirs (class 3) were derived from ponds (class 1) and small-sized reservoirs (class 2),

HESSD
9, 4001–4043, 2012

respectively. The results indicated that the annual water supplies from ponds (class 1), small-sized reservoirs (class 2) and small-sized reservoirs (class 3) are 9.79×10^6 m^3, 6.62×10^6 m^3, and 9.39×10^6 m^3, respectively.

4.3 Discussions

The results indicate that the simulation precision is improved at all four hydrologic stations in the improved SWAT2005 relative to the original SWAT2005. There is a clear improvement in the simulation of the Panshi and Dongfeng hydrologic stations, while the simulation of the Yangzishao and Wudaogou hydrologic stations improved less significantly over the validation periods. There is a clear improvement in the simulation of the Panshi and Dongfeng hydrologic stations, while the simulation of the Yangzishao and Wudaogou hydrologic stations improved less significantly for the flood seasons over the validation periods. The Panshi and Dongfeng hydrologic stations are located in the upper stream region of the Fengman Reservoir Basin, and water storages are the main human activities within their drainages. The Yangzishao and Wudaogou hydrologic stations are located in the lower stream region of the Fengman Reservoir Basin, and multiple human activities influence the hydrologic cycle within their drainages. Therefore, the simulation precision improved more at the Panshi and Dongfeng hydrologic stations. The improvements over the validation periods are mostly due to the improvements in the flood seasons over the validation periods, and the improvements in the flood seasons over the validation periods are mainly due to the consideration of the water balance and transport through a network combining both sequential and parallel streams and storage links.

The two-stage parameter calibration strategy and the three scenarios are used to compare the performances of the original and improved SWAT2005 in the regions with numerous small- and middle-sized water storages. The results indicate that using the improved SWAT2005, water balance and transport through a network combining both sequential and parallel streams and storage links reflects the basin charateristics reasonably well and significantly improves the precision of the simulation, especially in the

HESSD
9, 4001–4043, 2012

flood seasons. Through calibrating the physical and human activity parameters, the observed flows and simulated flows correspond well.

5 Conclusions

It becomes increasingly difficult to hydrologically simulate a catchment with a large number of water storages. In this paper, an improved version of SWAT2005 was developed to consider water storages with all of the available information in the basin hydrological simulation. The main characteristics of this model are summarised as follows: (1) a realistic representation of the relationships between the water surface area and volume of each type of water storages, ranging from small-sized ponds for water flow regulation to large- and medium-sized reservoirs for water supply and hydropower generation, (2) water balance and transport through a network combining both sequential and parallel streams and storage links, and (3) calibrations for the physical parameters and then the human interference parameters.

The two-stage parameter calibration strategy and the three scenarios are used to compare the performance between the original and improved SWAT2005 in the regions with numerous small- and medium-sized water storages. Compared to the original SWAT2005, the precision of the simulation during the stable period is improved at each hydrologic station in the improved SWAT2005. The results indicate that using the improved SWAT2005, water balance and transport through a network combining both sequential and parallel streams and storage links reflects the basin charateristics reasonably well and significantly improves the precision of the simulation, especially in the flood seasons. Through calibrating the physical and human activity parameters, the observed flows and simulated flows correspond well.

Therefore, compared to the original SWAT2005, the small- and medium-sized water storages are accurately modelled in the improved SWAT2005, which can be used in other basins or regions similar to the Fengman Reservoir Basin, particularly in the northeast of China, where there is a large number of water storages.

HESSD
9, 4001–4043, 2012

Acknowledgements. We are pleased to acknowledge the financial support for this project from the National Natural Science Foundation of China entitled Research on Laws of the Impacts of Human Activities on Catchment Water Cycle Based on SWAT Model (Grant No. 51079014) and the National Natural Science Foundation of China entitled Hydropower Reservoir Optimal Operation under Hydrometeorological Uncertain Enviroment (Grant No. 51109025). We would also like to thank the Institute of Water Resources and Flood Control of Dalian University of Technology in China for providing the data essential for this research.

References

Arnold, J. G. and Fohrer, N.: SWAT2000: current capabilities and research opportunities in applied watershed modelling, Hydrol. Process., 19(3), 563–572, 2005.

Borah, D. K. and Bera, M.: Watershed-scale hydrologic and nonpoint-source pollution models: review of applications, T. ASAE, 47(3), 789–803, 2004.

Chorography Editorial Committee of Jilin Province: Jilin Province Chorography Population, Jilin People's Publishing House, Changchun, 1991.

Frazier, P. S. and Page, K. J.: Water body detection and delineation with Landsat TM data, ISPRSJ. Photogramm. Eng. Remote Sens., 66(12), 1461–1467, 2000.

Gardini, B., Graf, G., and Ratie, G.: The instruments on Envisat. Acta Astronaut., 37, 301–311, 1995.

Gassman, P. W., Reyes, M. R., Green, C. H., and Arnold, J. G.: The soil and water assessment tool: historical development, applications, and future research directions, T. ASABE, 50(4), 1211–1250, 2007.

Gross, E. J. and Moglen, G. E.: Estimating the hydrological influence of Maryland state dams using GIS and the HEC-1 model, J. Hydrol. Eng., 12, 690–693, 2007.

Güntner, A., Krol, M. S., De Araújo, J. C., and Bronstert, A.: Simple water balance modelling of surface reservoir systems in a large data-scarce semiarid region, Hydrol. Sci. J., 49(5), 901–918, 2004.

Hao, F., Cheng, H., and Yang, S.: Non-Point Source Pollution Model, China Environmental Science Press, Beijing, 2006.

Hotchkiss, R. H., Jorgensen, S. F., Stone, M. C., and Fontaine, T. A.: Regulated river modeling for climate change impact assessment: the Missouri River, J. Am. Water Resour. Assoc., 36(2), 375–386, 2000.

HESSD

9, 4001–4043, 2012

Jayatilaka, C. J., Sakthivadivel, R., Shinogi, Y., Makin, I. W., and Witharana, P.: A simple water balance modelling approach for determining water availability in an irrigation tank cascade system, J. Hydrol., 273, 81–102, 2003.
Kannan, N., White, S. M., Worrall, F., and Whelan, M. J.: Sensitivity analysis and identification of the best evapotranspiration and runoff options for hydrological modeling in SWAT-2000, J. Hydrol., 332, 456–466, 2007.
Kuang, W. H., Zhang, S. W., Zhang, Y. Z., Li, Y., and Hou, W.: Changes of forest landscape and its driving mechanism during the last fifty years in the eastern mountain area of Jilin Province, J. Beijing Forest. Univ., 28(3), 38–45, 2006.
Liebe, J. R., Van De Giesen, N., and Andreini, M.: Estimation of small reservoir storage capacities in a semi-arid environment. A case study in the upper east region of Ghana, Phys. Chem. Earth, 30, 448–454, 2005.
Liebe, J. R., Van De Giesen, N., Andreini, M., Walter, M. T., and Steenhuis, T. S.: Determining watershed response in data poor environments with remotely sensed small reservoirs as runoff gauges, Water Resour. Res., 45, W07410, doi:10.1029/2008WR007369, 2009.
Lopez-Moreno, J. I., Vicente-Serrano, S. M., Begueria, S., Garcia-Ruiz, J. M., and Portela, M. M.: Dam effects on droughts magnitude and duration in a transboundary basin: the Lower River Tagus, Spain and Portugal, Water Resour. Res., 45, W02405, doi:10.1029/2008WR007198, 2009.
Luo, Y., He, C., Sophocleous, M., Yin, Z., Ren, H., and Zhu, O.: Assessment of crop growth and soil water modules in SWAT2000 using extensive field experiment data in an irrigation district of the Yellow River Basin, J. Hydrol., 352, 139–156, 2008.
McFeeters, S. K.: The use of the normalized difference water index (NDWI) in the delineation of open water features, Int. J. Remote Sens., 17(7), 1425–1432, 1996.
Mialhe, F., Gunnell, Y., and Mering, C.: Synoptic assessment of water resource variability in reservoirs by remote sensing: General approach and application to the runoff harvesting systems of south India, Water Resour. Res., 44, W05411, doi:10.1029/2007WR006065, 2008.
Mishra, A., Froebrich, J., and Gassman, P. W.: Evaluation of the SWAT model for assessing sediment control structures in a small watershed in India, T. ASABE, 50(2), 469–477, 2007.
Moriasi, D. N., Arnold, J. G., Van Liew, M. W., Bingner, R. L., Harmel, R. D., and Veith, T. L.: Model evaluation guidelines for systematic quantification of accuracy in watershed simulations, T. ASABE, 50(3), 885–900, 2007.
Neitsch, S. L., Arnold, J. G., Kiniry, J. R., Srinivasan, R., and Williams, J. R.: Soil and water

HESSD
9, 4001–4043, 2012

assessment tool user's manual. Version 2000, Texas Water Resources Institute, College Station, 412 pp., 2002a.
Neitsch, S. L., Arnold, J. G., Kiniry, J. R., Williams, J. R., and King, K. W.: Soil and water assessment tool theoretical documentation. Version 2000, Texas Water Resources Institute, College Station, 458 pp., 2002b.
Payan, J. L., Perrin, C., Andréassian, V., and Michel, C.: How can man-made water reservoirs be accounted for in a lumped rainfall-runoff model?, Water Resour. Res., 44, W03420, doi:10.1029/2007WR005971, 2008.
Saxton, K. E. and Willey, P. H.: Agricultural wetland and pond hydrologic analyses using the SPAW model, in: Self-Sustaining Solutions for Streams, Wetlands, and Watersheds (12–15 September 2004, St. Paul, Minnesota, USA), edited by: D'Ambrosio, J. L. and St. Joseph, Michigan, ASAE, ASAE Pub #701P0504, 16–23, 2004.
Sophocleous, M. A. and Perkins, S. P.: Methodology and application of combined watershed and ground-water models in Kansas, J. Hydrol., 236, 185–201, 2000.
Srinivasan, R., Arnold, J. G., Rosenthal, W., and Muttiah, R. S.: Hydrological modeling of Texas gulf Basin using GIS, in: GIS and Environmental Modeling: Progress and Research Issues, edited by: Goodchild, M. F., Steyaert, L. T., Parks, B. O., Johnston, C., Maidment, D., Crane, M., and Glendinning, S., GIS World Book, Fort Collins, 213–217, 1996.
Statistical Bureau of Jilin Province: Jilin Province Statistical Annual (2000), China Statistics Press, Beijing, 2001.
Van Liew, M. W., Garbrecht, J. D., and Arnold, J. G.: Simulation of the impacts of flood retarding structures on streamflow for a watershed in SouthWestern Oklahoma under dry, average, and wet climatic conditions, J. Soil Water Conserv., 58(6), 340–348, 2003.
Wang, G. and Xia, J.: Improvement of SWAT2000 modelling to access the impact of dams and sluices on streamflow in the Huai River basin of China, Hydrol. Process., 24, 1455–1471, 2010.
White, K. L. and Chaubey, I.: Sensitivity analysis, calibration, and validations for a multisite and multivariable SWAT model, J. Am. Water Resour. Assoc., 41(5), 1077–1089, 2005.
White, M. E.: Reservoir surface area from Landsat imagery, ISPRSJ. Photogramm. Eng. Remote Sens., 44(11), 1421–1426, 1978.
Zhang, S. W., Zhang, Y. Z., Li, Y., and Chang, L. P.: Analysis of spatial-temporal features of land use/cover change in Northeast, Science Press, Beijing, 2006.

HESSD
9, 4001–4043, 2012

Table 1. Classification of water storages and the total drainage area and storage volume of each class in the Fengman Reservoir Basin.

Class	1	2	3	4	5	Total
Storage capacity (10^6 m^3)	< 0.1	0.1–1.0	1.0–10.0	10.0–50.0	> 50.0	
Total drainage area (km^2)	2252	1989	1902	730	548	7421
Total storage volume (10^6 m^3)	54.62	152.63	255.07	179.82	316.00	958.14

HESSD
9, 4001–4043, 2012

Table 2. Classification of water storages and correlations between the water surface area (A; m^2) and principal storage volume (V; 10^4 m^3) of each water storage class within the basin.

Classification indexes			
Slope (%)	Drainage area (km^2)/principal storage volume(10^4 m^3)	Principal storage volume (10^4 m^3)	Correlation coefficient between A and V
0–15	≥0.14	≥10	0.80
		0–10	
	<0.14	≥ 10	0.74
> 15	≥ 0.1	≤17	0.90
		17–77	0.63
		≥77	0.73
	< 0.1	<77	0.63
		≥77	0.73

HESSD
9, 4001–4043, 2012

Table 3. Calibrated physical parameters.

Parameter name	Original value	Calibrated value
Alpha_Bf	0.048	0.200
ESCO	0.95	0.98
Gw_Delay	31	15
SFTMP	1.00	0.73
SMTMP	0.500	4.441
SMFMX	4.500	3.136
TIMP	1.000	0.048
CANMX		2.8 (crop) 4.8 (forest) 4.1 (grass)

HESSD
9, 4001–4043, 2012

Table 4. Calibrated human activity parameter values, including the principal storage volume adjustment parameters and the fraction parameters for different water sources.

Calibrated principal storage volume adjustment parameter values				
Parameter	$\beta_{fld,beg}$	$\beta_{fld,mid}$	$\beta_{fld,end}$	$\beta_{nonflod}$
Calibrated value	0.9	1.0	1.1	1.0
Calibrated fraction parameter values for different water sources				
Parameter	$\alpha_{pnd,maysep}$	$\alpha_{rch,maysep}$	$\alpha_{gw,maysep}$	
Calibrated value	0.587	0.391	0.022	
Parameter	$\alpha_{pnd,octapr}$	$\alpha_{rch,octapr}$	$\alpha_{gw,octapr}$	
Calibrated value	0.0	0.0	1.0	

HESSD
9, 4001–4043, 2012

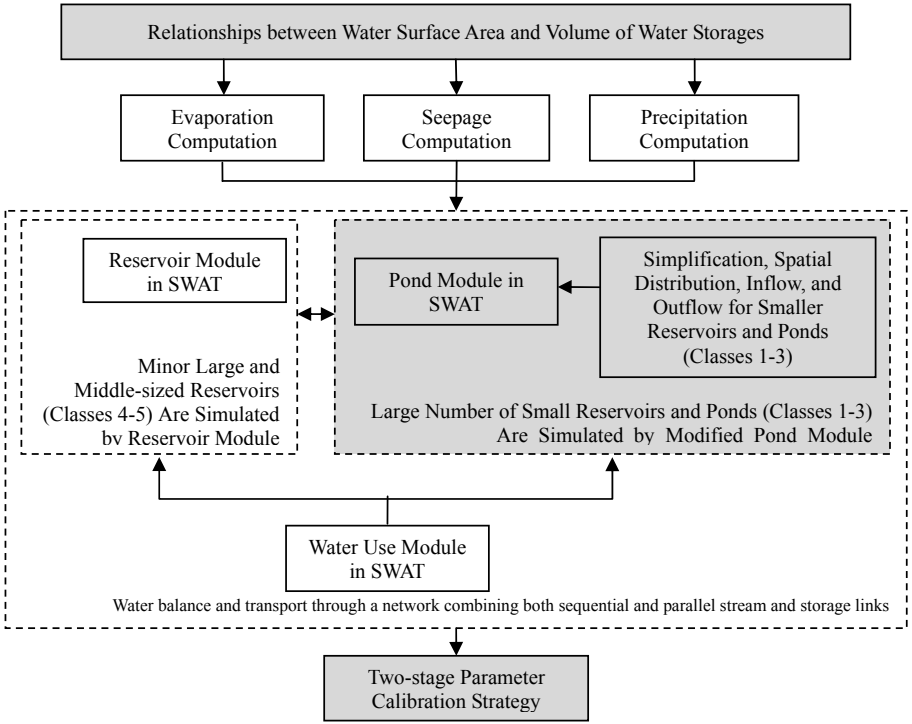

Fig. 1. Framework for the improved SWAT2005.

HESSD
9, 4001–4043, 2012

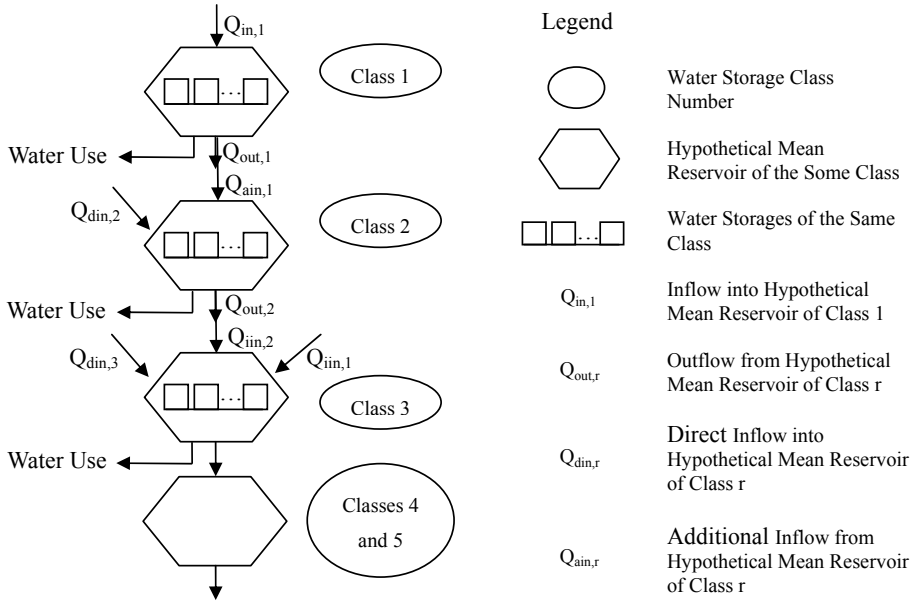

Fig. 2. Sequential and parallel routing scheme for water storages in the improved SWAT2005.

HESSD
9, 4001–4043, 2012

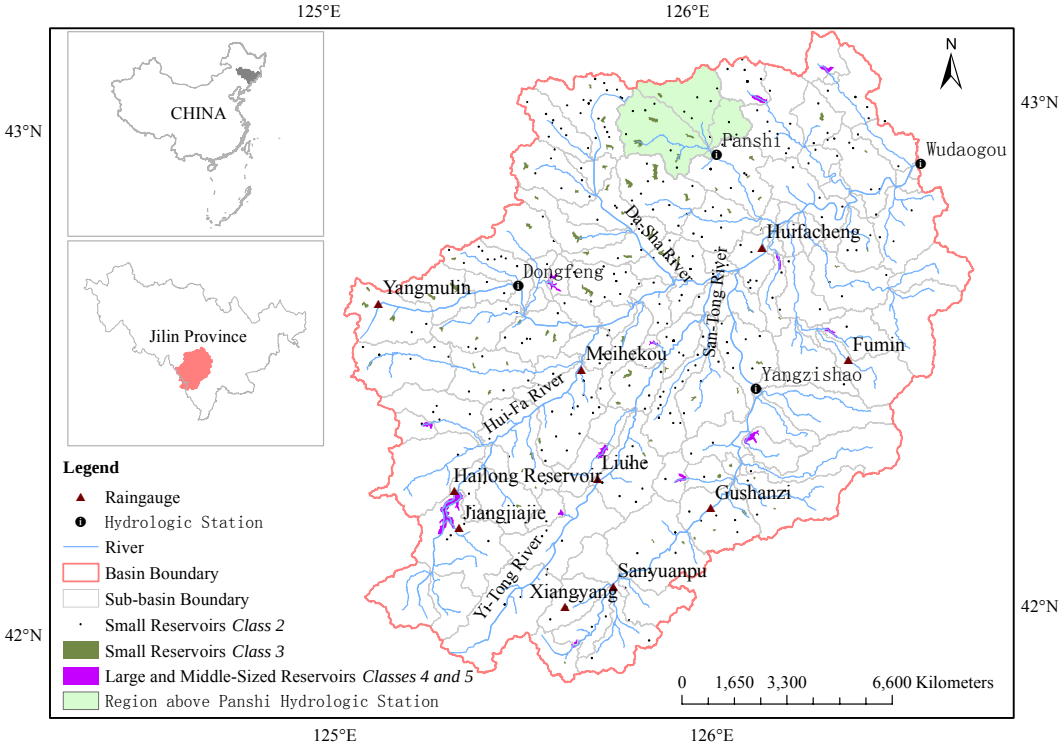

Fig. 3. The Fengman Reservoir Basin.

HESSD
9, 4001–4043, 2012

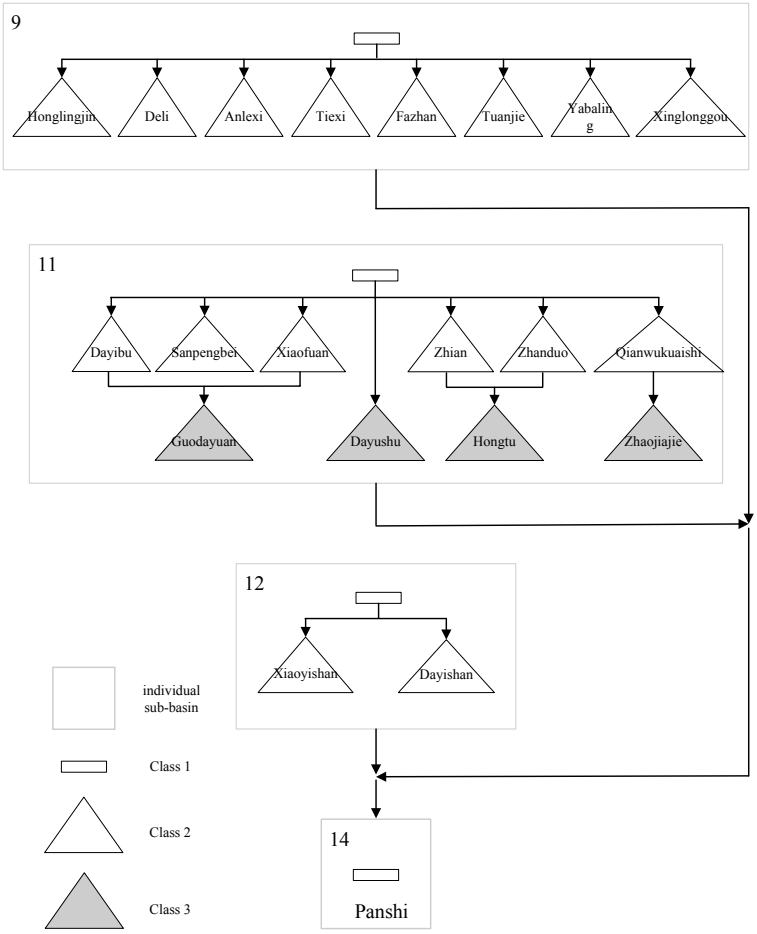

Fig. 4. Spatial topology of the water storages in the Panshi sub-basin.

HESSD
9, 4001–4043, 2012

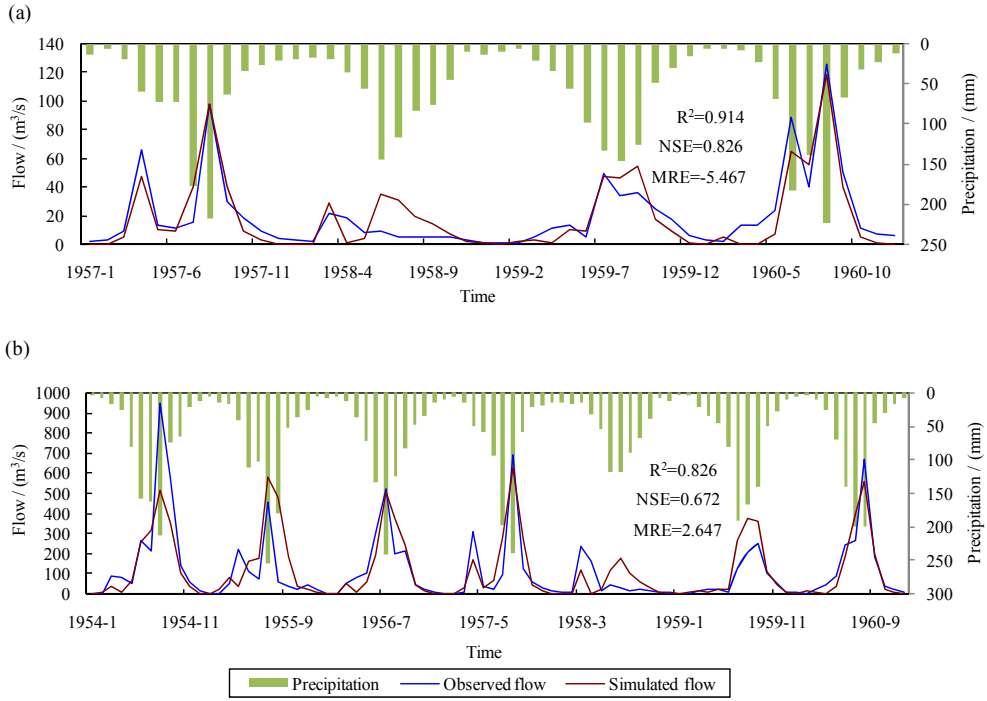

Fig. 5. Observed and simulated monthly streamflows during the physical parameter calibration period (before 1960) at two discharge gauges: **(a)** Yangzishao and **(b)** Wudaogou, where R^2 is the coefficient of determination; NSE is the Nash-Sutcliffe efficiency; and MRE (%) refers to the mean relative error.

HESSD
9, 4001–4043, 2012

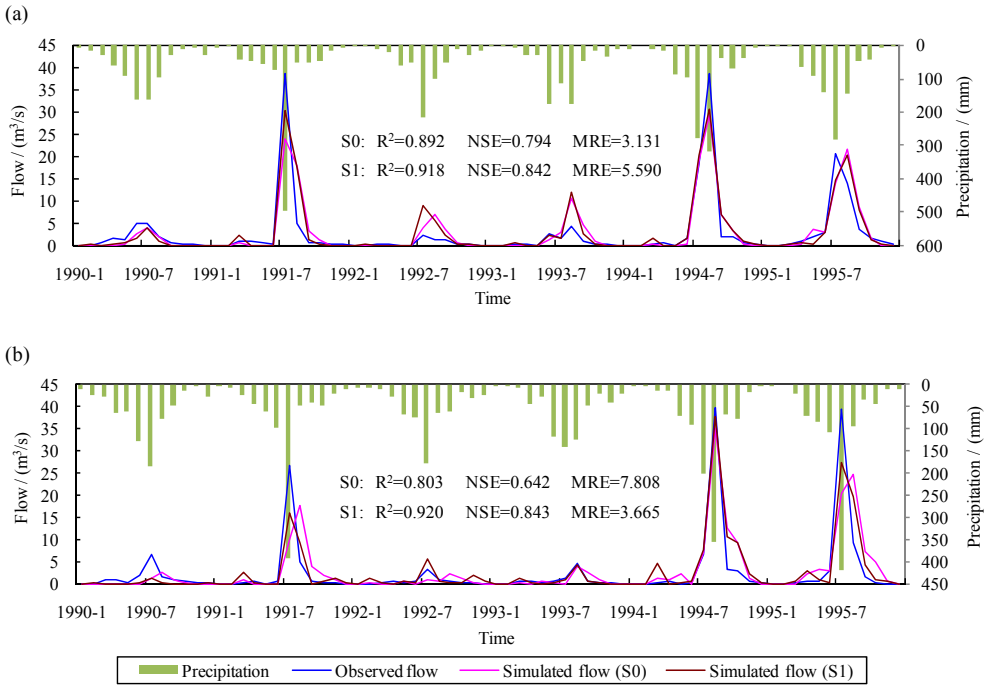

Fig. 6. Observed and simulated monthly streamflows during human activity parameter calibration period (1990–1995) at two discharge gauges: **(a)** Panshi and **(b)** Dongfeng. S0 refers to the consideration of human activities by the original SWAT2005 with calibrated physical parameters, while S1 refers to the consideration of human activities by the improved SWAT2005 with the calibrated physical and human activity parameters described above.

HESSD
9, 4001–4043, 2012

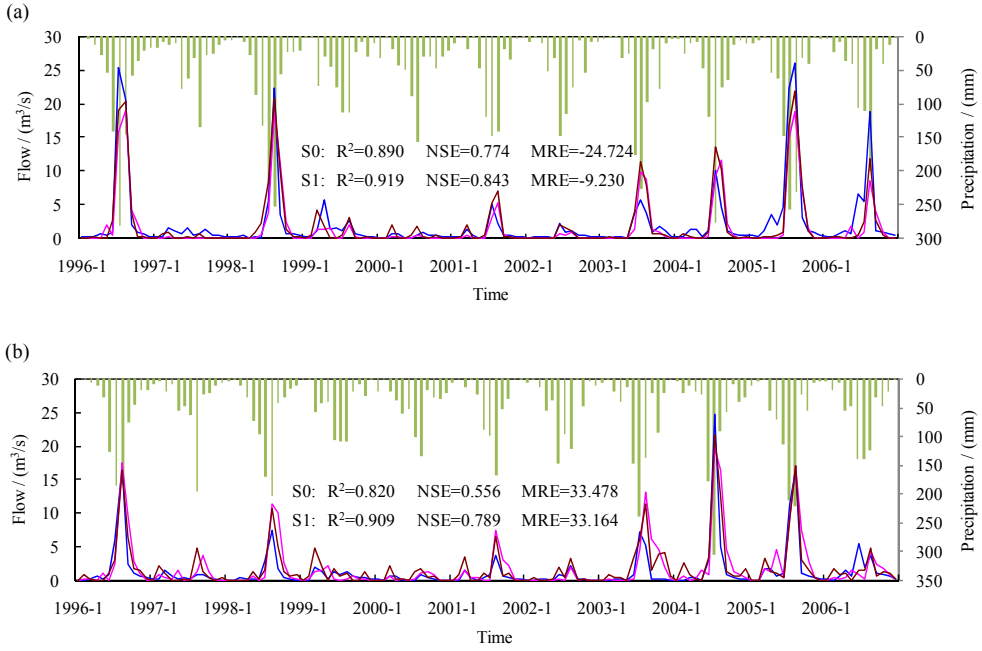

Fig. 7. Observed and simulated monthly streamflows over the validation periods at all four discharge gauges: **(a)** Panshi (1996–2006), **(b)** Dongfeng (1996–2006), **(c)** Yangzishao (1990–2006) and **(d)** Wudaogou (1990–2006).

HESSD
9, 4001–4043, 2012

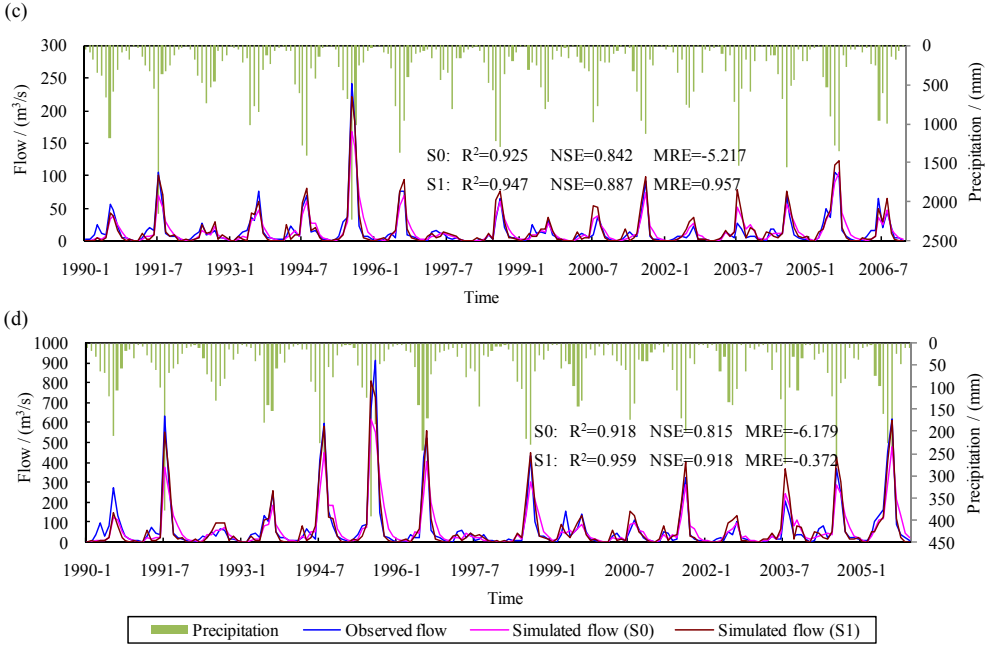

Fig. 7. Contined.

HESSD
9, 4001–4043, 2012

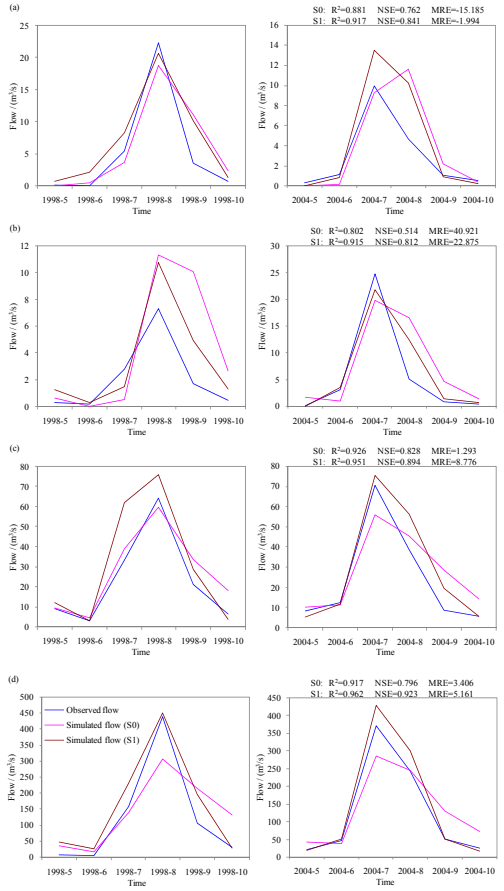

Fig. 8. Observed and simulated monthly streamflows for the 1998 and 2004 flood seasons at all four discharge gauges: **(a)** Panshi, **(b)** Dongfeng, **(c)** Yangzishao and **(d)** Wudaogou, where the evaluation criteria (R^2, NSE, and MRE) within each sub-figure refer to all of the flood seasons over the validation periods.

HESSD
9, 4001–4043, 2012

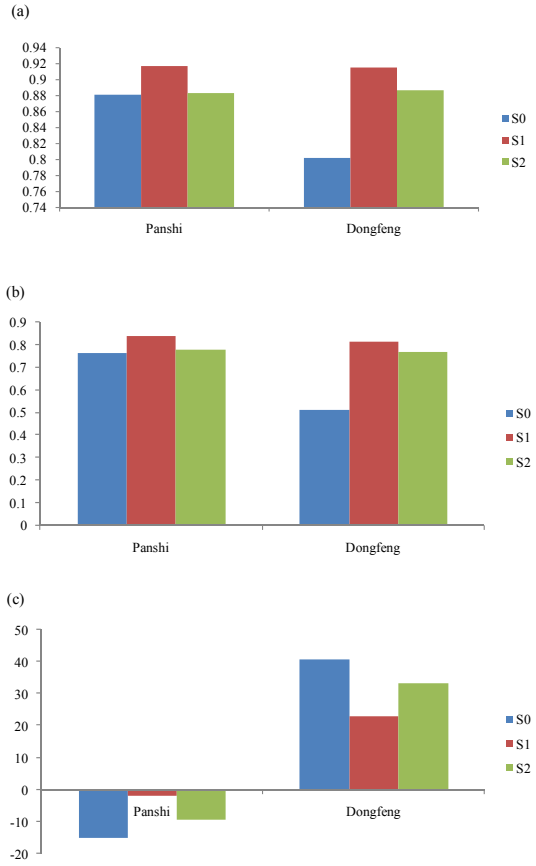

Fig. 9. Comparisons of the evaluation criterions for the flood seasons over the validation periods: **(a)** R^2, **(b)** NSE and **(c)** MRE. In S2, considering the water balance and transport through a network combining both sequential and parallel streams and storage links while ignoring the human activity parameters.

HESSD
9, 4001–4043, 2012

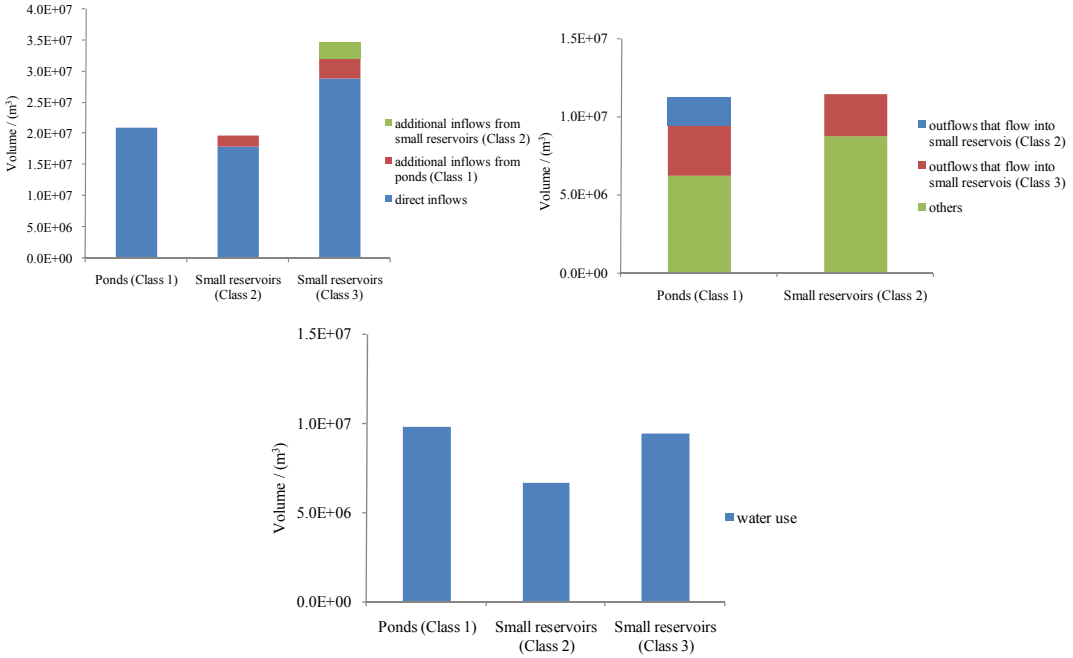

Fig. 10. Water balance and transport through a network combining both sequential and parallel streams and storage links above Panshi hydrologic station over the validation periods: **(a)** inflow, **(b)** outflow and **(c)** water use.

HESSD
9, 4001–4043, 2012